

A combined ion-sputtering and electron-beam annealing device for the in vacuo postpreparation of scanning probes

Georg Eder, Stefan Schlögl, Klaus Macknapp, Wolfgang M. Heckl, and Markus Lackinger


Citation: [Review of Scientific Instruments](#) **82**, 033701 (2011); doi: 10.1063/1.3556443

View online: <http://dx.doi.org/10.1063/1.3556443>

View Table of Contents: <http://scitation.aip.org/content/aip/journal/rsi/82/3?ver=pdfcov>

Published by the [AIP Publishing](#)

Advertisement:



The advertisement features the saes group logo on the left, which consists of the word "saes" in white lowercase letters above the word "group" in white lowercase letters, both on a red square background. To the right of the logo are four cylindrical, metallic-looking devices mounted on red square bases. Each device has a complex, perforated top section and a flange-like base. The devices are arranged in a cluster, with one in the foreground and three behind it. The background is a light gray gradient.

neg_technology@saes-group.com
www.saesgroup.com

A combined ion-sputtering and electron-beam annealing device for the *in vacuo* postpreparation of scanning probes

Georg Eder,¹ Stefan Schlögl,¹ Klaus Macknapp,² Wolfgang M. Heckl,^{2,3} and Markus Lackinger^{1,2}

¹Department of Earth and Environmental Sciences and Center for NanoScience (CeNS), Ludwig-Maximilians-University, Theresienstrasse 41, 80333 Munich, Germany

²Deutsches Museum, Museumsinsel 1, 80538 Munich, Germany

³Department of Physics, TUM School of Education, Technical University Munich, Schellingstrasse 33, 80333 Munich, Germany

(Received 29 November 2010; accepted 29 January 2011; published online 1 March 2011)

We describe the setup, characteristics, and application of an *in vacuo* ion-sputtering and electron-beam annealing device for the postpreparation of scanning probes (e.g., scanning tunneling microscopy (STM) tips) under ultrahigh vacuum (UHV) conditions. The proposed device facilitates the straightforward implementation of a common two-step cleaning procedure, where the first step consists of ion-sputtering, while the second step heals out sputtering-induced defects by thermal annealing. In contrast to the standard way, no dedicated external ion-sputtering gun is required with the proposed device. The performance of the described device is demonstrated by SEM micrographs and energy dispersive x-ray characterization of electrochemically etched tungsten tips prior and after postprocessing. © 2011 American Institute of Physics. [doi:10.1063/1.3556443]

I. INTRODUCTION

For scanning probe microscopy experiments the scanning probe, e.g., the metal tip for STM, is of pivotal importance. The tip is crucial for the stability of the tunneling current, and can thus be decisive for the noise levels of both signal and data. Yet, since the STM imaging process convolutes geometric and electronic properties of sample and tip, the probe also has a great impact on the contrast in high-resolution topographs, and similarly on spectroscopic data. Although the atomic configuration at the apex can normally not be controlled, at least the chemical cleanliness of the tips should be guaranteed. For the majority of STM experiments under UHV conditions tungsten is still the material of choice for the tip, not at least because electrochemical etching techniques for sharp tips are well developed.^{1,2} The mechanical properties of tungsten and its high melting point definitely render the material suitable; however, electrochemically etched tungsten tips are prone to oxidation under ambient conditions.^{1,2} Oxidized tungsten tips can result in unstable tunneling conditions and poor image quality, or the insulating oxide coating can even cause tip crashes during coarse approach.³ In order to remove not only tungsten-oxide layers but also etching remnants and byproducts, various procedures are proposed in the literature like annealing by electron bombardment,^{4,5} ion-sputtering,^{6–8} dipping into hydrofluoric acid (HF),⁹ and self-sputtering in a noble gas environment.¹⁰ Although it is difficult to establish a clear correlation between a specific postpreparation procedure and achieved quality of STM data, there is a consensus that an appropriate after-treatment improves the overall performance of STM tips.³ For STM experiments under UHV conditions the standard tip after-treatment is *in situ* ion-sputtering and subsequent thermal annealing. For sample preparation most UHV systems are equipped with an ion-sputtering gun. Due to the opera-

tion principle of STM the sample surface and the tip point into opposite directions. Hence, either a manipulation mechanism to rotate the tip or a second (typically rather expensive) ion-sputtering gun is necessary. Here, as an alternative we present a versatile, inexpensive, easy to realize, and customizable setup for the *in vacuo* postpreparation of scanning probes. First the setup is described, and then we present a characterization of the device by measuring the ion current at the tip as a function of various parameters along with a finite element simulation of the electrostatic potential and field. Finally, we demonstrate the efficiency of the device by comparison of as-etched with postprocessed tungsten tips.

II. EXPERIMENTAL SETUP

The basic setup of the postpreparation device is depicted in Fig. 1(a) and consists of an axial arrangement of filament, ring, and tip. In this test setup the tip is held by a spring-loaded socket (accepting wire diameters from 0.35 to 0.55 mm). The UHV compatible setup is assembled on a 40 CF flange equipped with four SHV high-voltage feedthroughs (rated for up to 5 kV and 16.5 A). The filament is made from a tungsten wire (diameter 0.2 mm, 13 coils), where one end is grounded to the flange on the vacuum side, while the other end is connected to one of the feedthroughs. The ring (tungsten wire, wire diameter 0.2 mm, ring diameter ~10 mm) is not closed and both ends are likewise connected to SHV feedthroughs. The fourth feedthrough is connected to the tip (holder). The heights of ring and filament on the axis are adjustable and distances are set to 12 mm between tip and ring, and 16 mm between ring and filament for the experiments described. The proposed basic setup can easily be customized to a specific tip transfer and carrier system. Figure 1(b) presents a sketch of a conceivable (not realized) adaptation of the

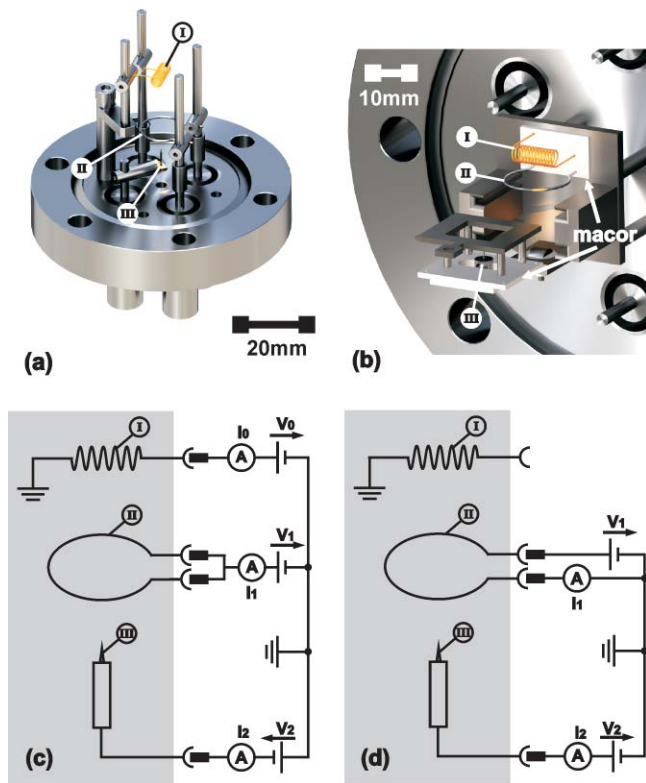


FIG. 1. (Color online) (a) Scheme of the combined ion-sputtering and electron-beam annealing device: (I) filament, (II) ring used as grid for ion-sputtering and used as a filament for electron-beam annealing, and (III) tip holder. (b) Adaptation scheme of the proposed device for Omicron tip holders. (c) Wiring diagram for the ion-sputtering mode: V_0 = filament voltage, V_1 = acceleration voltage for electrons, V_2 = acceleration voltage for noble gas ions, I_0 = filament current, I_1 = electron emission current, I_2 = ion current (d) Wiring diagram for the electron-beam annealing mode: V_1 = filament voltage, V_2 = acceleration voltage for electrons, I_1 = filament current, I_2 = electron emission current.

device for standard Omicron tip holders. The base plate of this slightly adapted Omicron tip holder is now made from macor—a machinable sinter ceramic. Also, the standard glued-on magnet is replaced by a mechanically clamped magnet with high Curie temperature, in order to prevent it from falling off or demagnetization during tip annealing. The tip is elec-

trically contacted from below with a sliding contact. The upper plate of the Omicron tip holder exhibits a wide cutout to avoid charging effects. The dimension and material of filament and ring are identical to the actually tested setup in Fig. 1(a). Ring and filament assemblies are fixed by setscrews in an insulating macor block and contacted from behind to electrical feedthroughs. This macor block is mounted onto a stainless steel fixture. The tip preparation stage can simply be loaded and unloaded by manipulation of Omicron tip holders into mountings on the side. Comparable adaptations are conceivable to any systems which feature tip exchange.

The proposed device can be operated in two different modes: ion-sputtering and electron-beam annealing. In order to alternate between these two modes, only the external wiring has to be changed, and respective wiring diagrams are depicted in Figs. 1(c) and 1(d).

For the ion-sputtering mode, a noble gas (typically neon or argon) has to be introduced into the vacuum chamber as the sputtering gas. Since most UHV systems are equipped with an ion-sputtering gun for sample preparation, the associated variable precision leak-valve can be used and no additional installations are required. After a partial noble gas pressure in the order of 10^{-5} mbar has been established, a dc current (~ 4.5 A) is passed through the filament, yielding thermal emission of electrons (~ 10 mA). While the filament is grounded, a positive voltage in the order of $+0.8$ kV is applied to the ring. Thermally emitted electrons are accelerated toward the ring and generate positive noble gas ions through impact ionization. In order to accelerate the positive ions toward the scanning probe, a negative voltage on the order of -2.0 kV is applied to the tip, resulting in a measurable ion current in the magnitude of microamperes. The ion current increases with both noble gas pressure and negative voltage on the tip as depicted in Fig. 2.

For ion-sputtering of tips with an external ion-sputtering gun best results are obtained when tips are mounted at the center of the ion beam.⁷ The required spherical symmetry is inherently achieved by design in our setup. Generally ion milling processes are dependent on many parameters such as the ion's angle of incidence,⁶ their kinetic energy, and their

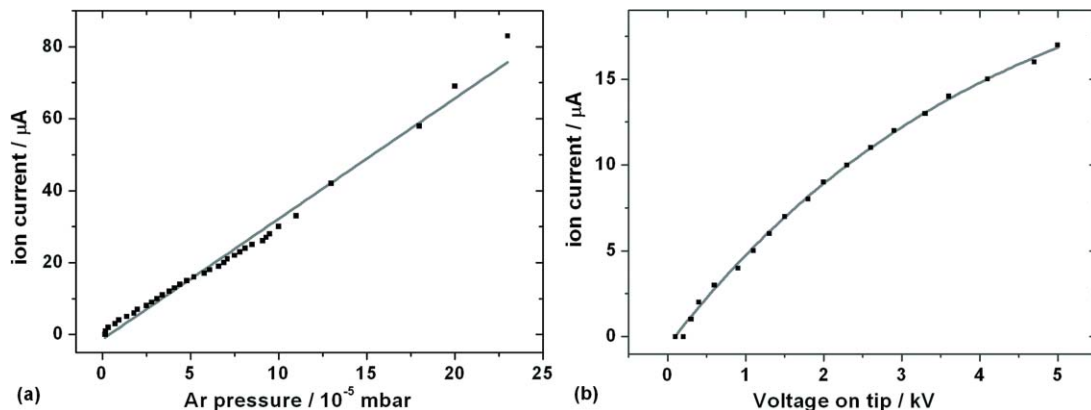


FIG. 2. Characteristics of the proposed device: (a) Ion current I_2 as a function of partial Ar pressure ($I_0 = 10$ mA (emission), $V_2 = -2.0$ kV (tip), V_1 (ring) was adjusted to keep I_0 (emission) constant). In the pressure range from 1×10^{-5} to 2.5×10^{-4} mbar the ion current as measured at the tip increases approximately linearly with Ar pressure, (b) ion current as a function of acceleration voltage at the tip ($p_{\text{Ar}} = 4 \times 10^{-5}$ mbar, $I_0 = 10$ mA (emission), V_1 (ring) adjusted to keep I_0 (emission) constant). An increasing negative extraction voltage at the tip results in sublinear increase of the ion current. Solid lines serve as guides to the eye.

chemical nature. In the proposed setup, the kinetic energy can easily be adjusted, while the angle of incidence apparently depends on the local surface orientation.

The second mode of the device is electron-beam annealing of the tip. For this purpose the ring which was used as a grid in the ion-sputtering mode is now used as filament, i.e., as a thermal electron source. As can be seen in the wiring diagram in Fig. 1(d) one side of the ring is grounded at the atmospheric side now, and a positive voltage on the order of +1.5 kV is applied to the tip. The ring when operated as a filament is heated by a dc current of ~ 4 A, resulting in an emission current of 1.5 mA as measured at the biased tip. The upper original filament is too remote to yield a reasonable electron current when a positive voltage is applied to the tip, possibly because of electrostatic screening through the ring. Annealing of sputtered STM tips is necessary to heal out sputtering-induced defects, yet, the annealing power as the product of emission current and applied voltage to the tip must not be too high to prevent melting-induced blunting of the apex.⁴ The enhancement of the electrostatic field due to the low radius of curvature at the tip leads to effective local heating of its apex.

For a quantitative understanding of the proposed device where a high positive voltage is applied to the ring and in close vicinity a high negative voltage is applied to the tip, a finite-element simulation of the electrostatic potential and electric field distribution were performed with the program package Ansoft's MAXWELL 2D.¹¹ Since an idealized setup exhibits rotational symmetry, resulting potential and field distributions are likewise rotational symmetric, and the 2D solution in the median plane represents a cross section of the 3D solution in the r - z plane. The geometry has been taken from the experiment, and simulation results for the ion-sputtering mode with -2.0 kV at the tip, $+0.8$ kV at the ring, and the filament grounded are depicted in Fig. 3. These simulations confirm

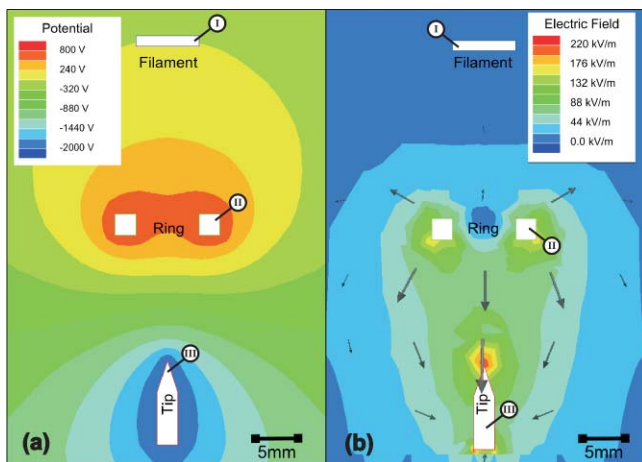


FIG. 3. (Color online) Finite element simulation results of (a) electrostatic potential and (b) electrostatic field (vectors and magnitudes) distributions for a 2D cross-sectional geometry of the device in the ion-sputtering mode with filament grounded, $+0.8$ kV at the ring, and -2.0 kV at the tip. These 2D maps represent a cross section of the rotational symmetric 3D solution in the r - z plane. Positively charged noble gas ions are generated above the ring by electron impact ionization, and are accelerated toward the tip by the electric field below the ring.

that the electric field vectors point toward the tip apex; hence, ions are accelerated to this region. Also the positively biased ring effectively screens the negative potential from the tip, and is thus able to attract electrons.

III. CHARACTERIZATION OF UNTREATED AND POSTPROCESSED STM TIPS

In order to demonstrate the efficiency of the proposed device, electrochemically etched tungsten tips were characterized by scanning electron microscopy (SEM, Zeiss LEO 440i) and spatially averaged energy dispersive x-ray (EDX) analysis. Topographs and spectra of the same tips were acquired directly after etching and compared to measurements acquired after ion-sputtering (Fig. 4) and annealing (Fig. 5). The STM tips were initially prepared by electrochemical ac etching of a polycrystalline tungsten wire (diameter 0.5 mm) in aqueous 2M KOH solution. In a second step, these tips were sharpened by electropolishing under optical control in a light microscope.¹² Ion-sputtering was performed with Ar^+ ions for 1 and 5 min, respectively, with the following parameters: $\sim 1.5 \times 10^{-5}$ mbar (3.1×10^{-5} mbar) Ar pressure, 4.0 A filament current, 10 mA electron emission current, $+830$ V ring voltage, -2.0 kV tip voltage. These values result in a stable ion current of $5 \mu\text{A}$ ($10 \mu\text{A}$) at the tip. Directly after electropolishing many tips exhibit not further identified, but clearly visible, contaminations [cf. Figs. 4(a) and 4(c)]. For about 50% of the tips, oxygen was detected by EDX at the foremost part, and attributed to the presence of tungsten oxide. These EDX-supported findings are in accordance with transmission electron microscopy studies by Garnæs *et al.*,¹³ who also concluded that electrochemically etched tungsten tips are covered with a few nanometer thick oxide layers. Similarly by means of EDX, aluminum was detected at the shank of the tip where the tungsten has not been

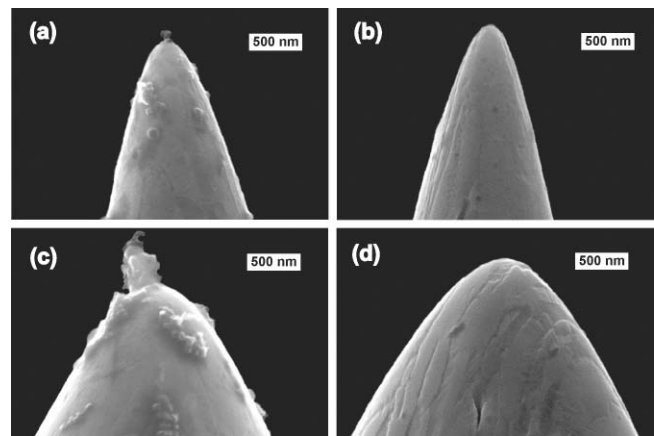


FIG. 4. SEM micrographs of electrochemically etched tungsten tips (a)/(c) directly after electrochemical etching and electropolishing without any further treatment, (b) the same tip as shown in (a) after sputtering with $5 \mu\text{A}$ for 1 min, (d) the same tip as shown in (c) after sputtering with $10 \mu\text{A}$ for 5 min. Both examples clearly demonstrate that ion-sputtering in the proposed device is efficient in removing contaminations, but also changes the surface structure, and possibly the tip shape. The tip shown in (d) was sputtered with a tenfold increased ion-dose as compared to (b), which already resulted in a detectable change of outer shape.

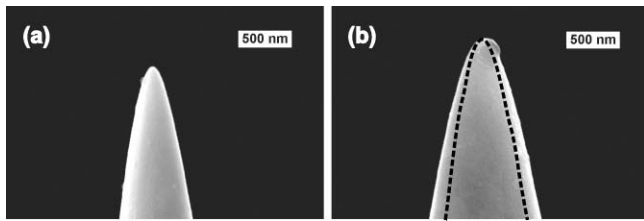


FIG. 5. SEM micrographs of an electrochemically etched tungsten tip (a) before and (b) after electron beam annealing (+1.5 kV, 1.5 mA, i.e., 2.25 W for 300 s). The outer shape of the tip before annealing has been reproduced in (b) by the dashed line, in order to illustrate the melting induced change of shape. The cone angle changes from 20° to 25° .

electrochemically etched. These contaminations might originate from the wire drawing process. After the postpreparation through ion-sputtering each tip was characterized again by SEM and EDX [cf. Figs. 4(b) and 4(d) for representative examples]. Apparently all contaminations have been removed and no oxide was detected anymore in the EDX spectra of ion-sputtered tips. As is evident from Fig. 4(d) the topography changes and the sputtered surfaces become rougher. Sputtering-induced surface roughening can be reduced by lowering the kinetic energy of the Ar^+ ions to 1 keV or less.⁷

Comparison of SEM images obtained for different sputtering times reveals this postpreparation method as a time critical process. The longer the sputtering time, the more material is removed. In order to smoothen the surface and heal out defects after the ion-sputtering treatment, cycles of heating are recommended.

Tip annealing was also found to be a time critical process, and moreover critical parameters for blunting are highly dependent on the initial microscopic shape of the tip, which is uncontrollably influenced not only by the electrochemical fabrication process but also by ion-sputtering. Typical parameters for tip annealing are high voltages around +1 kV, emission currents of ~ 1 mA, and a time span of minutes, where 1 min is more on the conservative side. SEM micrographs of an electropolished STM tip before and after annealing (+1.5 kV, 1.5 mA, 5 min) are depicted in Figs. 5(a) and 5(b), respectively. Comparison of the outer shapes reveals that this particular tip was already partly melted by the annealing process and became blunted. Even if the electrochemical etching procedure is carried out in a similar way with similar parameters, there is nevertheless a large scatter in the cone angle of the tips. Thus, it is difficult if not impossible to provide general parameters for annealing of tips. Nevertheless, we propose that for cone angles $\sim 25^\circ$, no indications of blunting were observable in SEM micrographs for annealing times < 3 min and currents of 1.5 mA at high voltages of +1.5 kV.

IV. CONCLUSION

We presented a device which can be used for both ion-sputtering and electron-beam annealing of STM tips without the need to change the hardware or manipulate the tip between both modes. Its performance is demonstrated by SEM images of sputtered tips which are free from previously detected contaminations, but exhibit clearly increased surface roughness. In addition, oxygen is absent in the EDX spectra of postprocessed tips, pointing toward complete removal of the tungsten oxide layer by the sputtering treatment.

Although self-sputtering (i.e., a high negative voltage applied to a sharp tip causes field emission; in a gas atmosphere, field emitted electrons can generate positive ions which are then accelerated toward the tip and sputter) is also a straightforward method to sputter STM tips, it imposes requirements on the tip. Only tips which are already sharp enough for field emission are suitable for self-sputtering. Since the proposed device also works for blunt tips it might be particularly useful to recover STM tips in UHV systems without a load lock and the possibility to introduce new tips.

ACKNOWLEDGMENTS

Financial support by the Nanosystems-Initiative Munich (NIM) is gratefully acknowledged. S.S. acknowledges financial support by Elitenetzwerk Bayern. G.E. is particularly grateful for financial support by the Hanns-Seidel-Stiftung. We would also like to thank Stephan Kloft for his help with the drawings.

- ¹J. P. Ibe, P. P. Bey, S. L. Brandow, R. A. Brizzolara, N. A. Burnham, D. P. DiLella, K. P. Lee, C. R. K. Marrian, and R. J. Colton, *J. Vac. Sci. Technol. A* **8**, 3570 (1990).
- ²A. D. Müller, F. Müller, M. Hietschold, F. Demming, J. Jersch, and K. Dickmann, *Rev. Sci. Instrum.* **70**, 3970 (1999).
- ³I. Ekvall, E. Wahlstrom, D. Claesson, H. Olin, and E. Olsson, *Meas. Sci. Technol.* **10**, 11 (1999).
- ⁴N. Ishida, A. Subagyo, A. Ikeuchi, and K. Sueoka, *Rev. Sci. Instrum.* **80**, 093703 (2009).
- ⁵Z. Q. Yu, C. M. Wang, Y. Du, S. Thevuthasan, and I. Lyubinetsky, *Ultramicroscopy* **108**, 873 (2008).
- ⁶P. Hoffrogge, H. Kopf, and R. Reichelt, *J. Appl. Phys.* **90**(10), 5322 (2001).
- ⁷S. Morishita and F. Okuyama, *J. Vac. Sci. Technol. A* **9**, 167 (1991).
- ⁸R. Zhang and D. G. Ivey, *J. Vac. Sci. Technol. B*, **14**, 1 (1996).
- ⁹E. Paparazzo, L. Moretto, S. Selci, M. Righini, and I. Farne, *Vacuum* **52**, 421 (1999).
- ¹⁰S. Ernst, S. Wirth, M. Rams, V. Dolocan, and F. Steglich, *Sci. Technol. Adv. Mat.* **8**, 347 (2007).
- ¹¹Ansoft MAXWELL 2D Version 9.0.573SV, Available: www.ansoft.com.
- ¹²J. T. Yates, *Experimental Innovations in Surface Science: A Guide to Practical Laboratory Methods and Instruments* (Springer-Verlag, New York, 1998).
- ¹³J. Garnaes, F. Kragh, K. A. Morch, and A. R. Tholen, *J. Vac. Sci. Technol. A* **8**(1), 441 (1990).